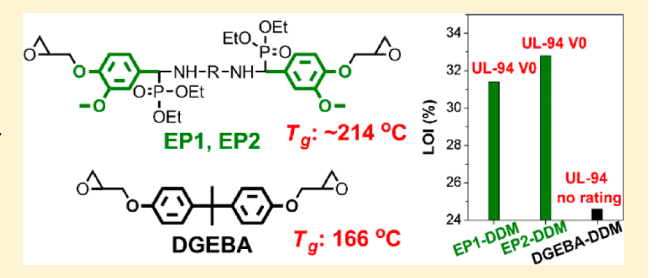
Macromolecules

Vanillin-Derived High-Performance Flame Retardant Epoxy Resins: **Facile Synthesis and Properties**

Sheng Wang,^{†,‡} Songqi Ma,*,^{†,‡} Chenxiang Xu,^{†,‡} Yuan Liu,^{†,‡} Jinyue Dai,^{†,‡} Zongbao Wang,[§] Xiaoqing Liu,[†] Jing Chen,[†] Xiaobin Shen,^{†,‡} Jingjing Wei,[†] and Jin Zhu*,[†]

ABSTRACT: Lignin derivative vanillin when coupled with diamines and diethyl phosphite followed by reaction with echichlorohydrin yields high-performance flame retardant epoxy resins. Biorenewable and environment-friendly flame retardant alternatives to bisphenol A epoxy resins (having plenty of applications such as coatings, adhesives, composites, etc.) have captured great attention due to their ecological and economic necessity. Vanillin, an industrial scale monoaromatic compound from lignin, is a promising sustainable candidate for highperformance polymers, while synthesis of diepoxies is challenging.



Meanwhile, bio-based epoxy resins combining high performance and excellent fire resistance are more difficult to be achieved. In this paper, two novel bio-based epoxy monomers EP1 and EP2 were synthesized by one-pot reaction containing Schiff base formation and phosphorus-hydrogen addition between vanillin, diamines, and diethyl phosphite, followed by reacting with epichlorohydrin. Their reactivities are similar to bisphenol A epoxy resin DGEBA. After curing they showed excellent flame retardancy with UL-94 V0 rating and high LOI of ~32.8%, which was due to the outstanding intumescent and dense char formation ability. Meanwhile, it was found that the cured vanillin-based epoxies had exceedingly high T_{o} s of ~214 °C, tensile strength of \sim 80.3 MPa, and tensile modulus of \sim 2709 MPa, much higher than the cured DGEBA with $T_{\rm g}$ of 166 °C, tensile strength of 76.4 MPa, and tensile modulus of 1893 MPa; the properties of vanillin-based epoxies are easy to be regulated by using different "coupling" agents—diamines—during the synthesis process.

INTRODUCTION

Epoxy resins, as one of the three most important thermosetting polymers, have been widely employed in a multitude of fields such as coatings, adhesives, laminated circuit board, electronic component encapsulations, and advanced composites because of their excellent adhesion, chemical resistance, mechanical properties, and dielectric properties. 1-5 Nowadays, almost all of the epoxy resins are produced from fossil resources, and 90% of the commercially available epoxy resins are diglycidyl ether of bisphenol A (DGEBA) via the reaction of bisphenol A with epichlorohydrin.⁶ Bisphenol A, fully dependent on fossil resources, accounts for greater than 67% of the molar mass of DGEBA.7 In addition, bisphenol A is a reprotoxic compound;⁸ and even if chemically incorporated into polymers, a small amount of bisphenol A can still release from the polymers with time due to the not completely stable chemical bonds linking bisphenol A.9 As a result, it is under close monitoring, and its application has been restricted in many countries.

Recently, the finite and rising price of fossil resources, climate change from CO₂ emission, and other environmental problems have raised interests in polymers from biorenewable raw materials which have a wide variety of biomass resources with low price and enhanced environment benefits. There are numerous bionewable resources including vegetable oils, 10-14 cardanol, 15 isosorbide, 9,16 rosin, 17,18 gallic acid, 19–21 ferulic acid, 22 lignin, and its derivatives 23–26 that have been investigated as feedstocks for epoxy resins. Because of the long flexible aliphatic chain and low reactivity of internal epoxy groups, epoxidized vegetable oil and cardanol often exhibit poor thermal and mechanical properties. 6,27 Although isosorbide, rosin, gallic acid, and ferulic acid-based epoxy resins exhibited satisfied thermal and mechanical properties, isosorbide-based one suffered from relatively high hydrophilicity,²⁸ and rosin, gallic acid, and ferulic acid have seldom spare capacity due to their variety applications and limited resources. Lignin is the second most abundant natural organic material accounting for approximately 30% of organic carbon in the biosphere; it is also the only scalable renewable feedstock consisted of aromatic monomers,²⁹ and it is highly underutilized.³⁰ Epoxy resins directly from lignin exhibit several drawbacks such as slow curing rate, unstable properties, and issues with processability

Received: January 16, 2017 Revised: February 20, 2017 Published: February 24, 2017

[†]Ningbo Institute of Materials Technology and Engineering, Chinese Academy of Sciences, 1219 Zhongguan West Road, Zhenhai District, Ningbo 315201, P. R. China

[‡]University of Chinese Academy of Sciences, 19 A Yuquan Rd, Shijingshan District, Beijing 100049, P. R. China

[§]Ningbo University, Ningbo 315201, P. R. China

due to their high molecular weights, insolubility, and composition variability depending on the species or the time of year, 30-32 which greatly limited their utilization. Despite a great deal of efforts, decomposition of lignin into small molecules remains a challenge. Fortunately, the lignin-tovanillin process has been commercially utilized, and vanillin, as the only monoaromatic compounds produced on an industrial scale from lignin, has already exhibited tremendous potential to be used as a renewable building block for polymers. 33,34 However, vanillin has only one group suitable to be introduce epoxy group; consequently, producing diepoxies is challenge. Oxidation or reduction of vanillin's formyl group was conducted to achieve two suitable groups to introduce two epoxy groups, 25,26 and using pentaerythritol reacting with formyl group and "coupling" two vanillin to achieve a difunctional phenol followed by reacting with epichlorohydrin is also a reported way to produce diepoxies.²³ These methods are relatively complex, and toxic compounds were utilized; the fundamental mechanical properties of the vanillin-based epoxies were not reported.

The second drawback of epoxy resins is their flammability, which blocks their application in the fire resistance required fields.³⁵ Phosphorus-containing compounds have been regarded as effective and environment-friendly flame retardants for polymers including epoxy resins, and phosphoruscontaining flame retardants have attracted intensive interests³⁶ after some halogenated fire retardants were banned by the European Union due to their toxicity.³⁷ Recent years have witnessed rapid development of phosphorus-containing epoxy resins, while most of the phosphorus-containing epoxy systems manifested a decrease in glass transition temperature (T_{σ}) than the phosphorus-free systems due to the limited chemical structure design and relatively low cross-link density of the cured epoxy resin.³⁸ Sustainability, reduction of environmental impacts, and green chemistry are increasingly guiding the development of phosphorus-containing materials from renewable resources,³⁹ while there is limited report on biobased phosphorus-containing epoxy resins.

Thus, in this paper, two novel high-performance flame retardant bio-based epoxy resins containing phosphorus were synthesized from vanillin. Diamines were used as the coupling agents in this work, and the Schiff base intermediates (produced from the coupling reaction between vanillin and diamines), without being extracted from the systems, further reacted with diethyl phosphite to obtain phosphorus-containing difunctional phenols; and then the flame retardant epoxy resins EP1 and EP2 were obtained by reacting these difunctional phenols with epichlorohydrin. The chemical structures of the monomers were characterized by FTIR, ¹H NMR, and ¹³C NMR. DDM was used to cure EP1, EP2, and DGEBA (the control) to obtain three thermosetting resins EP1-DDM, EP2-DDM, and DGEBA-DDM. The curing behaviors of the systems were examined by differential scanning calorimetry (DSC). Flame retardancy and flame retarding mechanism of the epoxy resins were investigated by vertical burning and limit oxygen index test and char analysis using inductively coupled plasma optical emission spectrometer (ICP-OES), X-ray photoelectron spectroscopy (XPS), and scanning electron microscopy (SEM). The thermal stability, glass transition temperature, and mechanical properties were studied by thermogravimetric analysis (TGA), DSC, and tensile test, respectively.

■ EXPERIMENTAL SECTION

Materials. Vanillin, 4,4-diaminodiphenylmethane (DDM), tetrabutylammonium bromide, *p*-phenylenediamine (PDA), and diethyl phosphite were purchased from Aladdin-reagent Co., China. Zinc chloride, epichlorohydrin (ECH), ethanol, petroleum ether, dichloromethane, and sodium hydroxide were obtained from Sinopharm Chemical Reagent Co., Ltd., China. Epoxy resin (DGEBA, trade name DER331, epoxy value 0.53) was supplied by DOW Chemical Company.

Synthesis of Tetraethyl(4,4'-methylenebis(4,1-phenylene)bis(azanediyl))bis((4-hydroxy-3-methoxyphenyl)methylene)diphosphonate (DP1). DP1 was synthesized by a quintessential condensation reaction between vanillin and 4.4-diaminodiphenylmethane, followed by an addition reaction with diethyl phosphite. 20 g (0.13 mol) of vanillin was dissolved in 150 mL of ethanol in a 500 mL three-neck flask equipped with a magnetic stirrer and a reflux condenser. 11.83 g (0.06 mol) of 4,4-diaminodiphenylmethane dissolved in 50 mL of ethanol was added dropwise into the flask over a period of 0.5 h at 25 °C, and they were reacted at 40 °C for 1 h. Then diethyl phosphite (24.86 g, 0.18 mol) and zinc chloride (0.5 g) as the catalyst for the addition reaction were added into the system, and the mixture was heated from 40 to 80 °C under a nitrogen atmosphere and kept at 80 °C for 8 h. Finally, the mixture was poured into 1000 mL of petroleum ether and stirred for 0.5 h after being cooled to room temperature. A white solid was collected by filtration; then the white crystalline product DP1 (29.7 g) with the yield of around 93.3% was obtained after being washed with ethanol twice followed by drying at 70 °C for 24 h in a vacuum oven. The synthetic route is illustrated in Scheme 1.

Scheme 1. Synthetic Routes of DP1 and DP2

FTIR (KBr), cm^{-1} : 3364 (N-H); 3225 (O-H); 1278 (P=O); 1026 (P-O).

 1 H NMR (DMSO- d_{6} , ppm): δ = 1.02 (t, 6H), 1.14 (t, 6H), 3.51 (d, 2H), 3.65 (m, 6H), 3.83 (m, 2H), 3.99 (m, 4H), 4.76 (dd, 2H), 5.96 (dd, 2H), 6.64 (dd, 6H), 6.75 (d, 4H), 6.84 (d, 2H), 7.07 (s, 4H), 8.85 (s, 2H).

¹³C NMR (DMSO- d_6 , ppm): δ = 16.68 (dd, 4C), 39.94 (s, 1C), 53.64 (s, 1C), 55.17 (s, 1C), 56.12 (s, 4C), 62.65 (dd, 2C), 113.09 (d, 2C), 114.07 (s, 4C), 115.40 (s, 2C), 121.38 (d, 2C), 128.00 (s, 2C), 129.18 (s, 4C), 130.78 (s, 2C), 145.76 (d, 2C), 146.34 (d, 2C), 147.69 (d, 2C).

Synthesis of Tetraethyl(1,4-phenylenebis(azanediyl))bis((4-hydroxy-3-methoxyphenyl)methylene)diphosphonate (DP2).

DP2 was also synthesized by a quintessential condensation reaction between vanillin and p-phenylenediamine followed by an addition reaction with diethyl phosphite. 20 g (0.13 mol) of vanillin was dissolved in 150 mL of ethanol in a 500 mL three-neck flask equipped with a magnetic stirrer and a reflux condenser. 6.4884 g (0.06 mol) of p-phenylenediamine dissolved in 50 mL of ethanol was added dropwise into the flask over a period of 0.5 h at 25 °C, and they were reacted at 40 °C for 1 h. Then diethyl phosphite (24.86 g, 0.18 mol) and zinc chloride (0.5 g) as the catalyst for the addition reaction were added into the system, and the mixture was heated from 40 to 80 °C under a nitrogen atmosphere and kept at 80 °C for 8 h. Finally, the mixture was poured into 1000 mL of H₂O and stirred for 0.5 h after being cooled to room temperature. A light yellow solid was collected by filtration; then the light yellow crystalline product DP2 (23.4 g) with the yield of around 88.3% was obtained after being washed with acetone twice followed by drying at 70 °C for 24 h in a vacuum oven. The synthetic route is illustrated in Scheme 1.

FTIR (KBr), cm⁻¹: 3390 (O-H, N-H); 1285 (P=O); 1040 (P-O).

 1 H NMR (DMSO- 2 G, ppm): δ = 1.02 (t, 6H), 1.16 (t, 6H), 3.62 (m, 2H), 3.71 (s, 6H), 3.82 (m, 2H), 4.00 (p, 4H), 4.65 (dd, 2H), 5.39 (dd, 2H), 6.51 (d, 4H), 6.64 (d, 2H), 6.81 (d, 2H), 7.05 (s, 2H), 8.84 (s, 2H).

(s, 2H). ¹³C NMR (DMSO- d_6 , ppm): δ = 16.68 (dd, 4C), 54.54 (s, 2C), 56.08 (s, 4C), 62.5 (m, 2C), 112.99 (s, 2C), 115.37 (s, 4C), 121.32 (s, 2C), 128.23 (s, 2C), 139.51 (d, 4C), 146.2 (s, 2C), 147.66 (s, 2C).

Synthesis of Tetraethyl(4,4'-methylenebis(4,1-phenylene)bis(azanediyl))bis((3-methoxy-4-(oxiran-2-ylmethoxy)phenyl)methylene)diphosphonate (EP1). 5 g of DP1 (0.0058 mol), 53.7 g of epichlorohydrin (0.58 mol), and 0.5 g of tetrabutylammonium bromide (10 wt % of DP1) as the catalyst were placed in a threenecked flask equipped with a magnetic stirrer and a reflux condenser, and the mixture was reacted at 80 °C for 3 h. After being cooled to 5 °C, 2.32 g of 40 wt % aqueous sodium hydroxide solution (0.058 mol NaOH) was added dropwise into the flask and reacted for 5 h. The solution was washed with distilled water three times after diluted with dichloromethane; then a light yellow solid was collected after removing dichloromethane and epichlorohydrin. Finally, the light yellow solid product EP1 (5.3 g) with the yield of around 93.5% was obtained after being washed with petroleum ether twice followed by drying at 50 °C for 24 h in a vacuum oven. The synthetic route is illustrated in Scheme 2.

FTIR (KBr), cm^{-1} : 3300(N-H); 1265 (P=O); 1027 (P-O); 910 (epoxy).

 1 H NMR (CDCl₃, ppm): δ = 1.07 (t, 6H), 1.27 (t, 6H), 2.72 (dd, 2H), 2.88 (t, 2H), 3.37 (s, 2H), 3.70 (m, 4H), 3.84 (s, 6H), 4.01 (m, 8H), 4.19 (dt, 2H), 4.62 (d, 2H), 6.47 (t, 4H), 6.91 (dd, 10H).

¹³C NMR (CDCl₃, ppm): δ = 16.38 (dd, 4C), 40.06 (s, 1C), 44.92 (s, 2C), 50.13 (s, 2C), 55.17 (s, 1C), 55.96 (s, 4C), 56.68 (s, 1C), 63.23 (d, 2C), 70.12 (s, 2C), 111.37 (s, 2C), 113.71 (s, 2C), 113.93 (s, 4C), 120.19 (d, 4C), 129.41 (s, 4C), 131.72 (s, 2C), 144.48 (s, 2C), 147.60 (s, 2C), 149.59 (s, 2C).

Synthesis of Tetraethyl(1,4-phenylenebis(azanediyl))bis((3methoxy-4-(oxiran-2-ylmethoxy)phenyl)methylene)diphosphonate (EP2). $5\ g$ of DP2 (0.0065 mol), $60.1\ g$ of epichlorohydrin (0.65 mol), and 0.5 g of tetrabutylammonium bromide (10 wt % of DP2) as the catalyst were placed in a threenecked flask equipped with a magnetic stirrer and a reflux condenser, and the mixture was reacted at 80 °C for 3 h. After being cooled to 5 °C, 2.6 g of 40 wt % aqueous sodium hydroxide solution (0.065 mol of NaOH) was added dropwise into the flask and reacted for 5 h. The solution was washed with distilled water three times after diluted with dichloromethane; then a light yellow solid was collected after removing dichloromethane and epichlorohydrin. Finally, the white solid product EP2 (4.3 g) with the yield of around 75.2% was obtained after being washed with petroleum ether twice followed by drying at 50 °C for 24 h in a vacuum oven. The synthetic route is illustrated in Scheme 2.

Scheme 2. Synthetic Routes of EP-1 and EP-2

FTIR (KBr), cm⁻¹: 3383 (N–H); 1264 (P=O); 1033 (P–O); 910 (epoxy).

¹H NMR (CDCl₃, ppm): δ = 1.14 (t, 6H), 1.27 (t, 6H), 2.74 (dd, 2H), 2.90 (t, 2H), 3.39 (s, 2H), 3.71 (m, 2H), 3.85 (s, 6H), 4.03 (m, 8H), 4.19 (dt, 2H), 4.55 (d, 2H), 6.43 (s, 4H), 6.92 (m, 6H).

¹³C NMR (CDCl₃, ppm): δ = 16.37 (dd, 4C), 44.95 (s, 2C), 50.11 (s, 2C), 55.98 (d, 4C), 57.52 (s, 2C), 63.16 (m, 2C), 70.10 (s, 2C), 111.30 (s, 2C), 113.61 (s, 2C), 115.45 (s, 4C), 120.18 (d, 2C), 129.62 (s, 2C), 139.24 (d, 2C), 147.55 (s, 2C), 149.54 (s, 2C).

Preparation of the Cured Epoxy Resins. Both EP1 and EP2 were cured with a commonly used curing agent DDM. Epoxy monomers were mixed with DDM in a 1:1 equiv ratio. The mixtures were cured by a plate vulcanizer at 200 °C for 3 min (1 min for removing bubbles, 2 min for heat pressing) to get films with thickness of approximately 100 μ m for thermal and mechanical properties examination. The mixtures were also melted and poured into stainless steel molds and cured at 160 °C for 2 h to obtain samples with dimensions of 80 mm × 6.5 mm × 3 mm for flame retardancy investigation. Both films and rectangular samples were postcured at 200 °C for 2 h and 230 °C for 2 h in a vacuum oven. For comparison, commonly used bisphenol A epoxy resin (DGEBA) was also cured with the same curing agent.

Characterization. ¹H NMR and ¹³C NMR spectra were recorded by an AVANCE III Bruker NMR spectrometer (Bruker, Switzerland) with DMSO-d₆ and CDCl₃ as solvents, operating at 400 and 75.5 MHz, respectively. The infrared spectra (FTIR) were measured with a NICOLET 6700 FTIR (NICOLET, America) using the KBr pellet method. Differential scanning calorimetry (DSC) measurements were performed under a nitrogen atmosphere on a Mettler Toledo Star 1 apparatus and a PerkinElmer DSC8000 apparatus for nonisothermal curing kinetics and glass transition temperature (T_g) , respectively. The mixtures (around 3-5 mg) of epoxy monomers and DDM were taken for the study of nonisothermal curing kinetics. A heat scan ranging from 50 to 250 °C was performed at varying heating rates of 5, 10, 15, and 20 °C min⁻¹, respectively. Cured samples (around 8–10 mg) were heated from 50 to 250 °C at a heating rate of 20 °C min⁻¹ and held at 250 °C for 3 min to eliminate thermal history, and then they were cooled to 50 °C at a cooling rate of 20 °C min $^{-1}$ followed by being heated again to 250 °C at a rate of 20 °C min⁻¹. The T_{σ} was obtained from the second heating curve of the cured epoxy resins. Cured samples with dimensions of 30 mm \times 0.5 mm \times 100 μ m were used to examine tensile properties by a Universal Mechanical Testing Machine (Instron 5569A) with a cross-head speed of 0.5 mm min⁻¹. The tensile properties of each sample were reported as the average of five

measurements. Thermogravimetric analysis (TGA) was carried using a Mettler-Toledo TGA/DSC1 thermogravimetric analyzer (METTLER TOLEDO, Switzerland). Approximately 3-5 mg samples were heated from 50 to 700 °C at a heating rate of 10 °C min⁻¹ under nitrogen and air atmospheres. The limit oxygen index (LOI) was obtained on a JF-3 oxygen index instrument (Jiangning Analysis Instrument Company, China) with sample dimensions of 80 mm × 6.5 mm × 3 mm according to ASTM D2863-10. UL-94 vertical burning tests were conducted according to ASTMD2863-97 on an AG5100B vertical burning tester (Zhuhai Angui Testing Equipment Company, China) with sample dimensions of 80 mm × 6.5 mm × 3 mm. The morphologies of residues collected after LOI tests were observed by scanning electron microscopy (SEM, EVO18) with an accelerating potential of 20 kV. DGEBA-DDM could not self-extinguish, so it was blown out during the test in order to investigate the morphology of its surface during the burning. The residues of phosphorus content after LOI tests were performed by inductively coupled plasma optical emission spectrometer (ICP-OES) on a PerkinElmer Optima 2100DV apparatus. 20 mL of aqua regia (10 mL of H₂O, 7.5 mL of HCl, and 2.5 mL of HNO₃) was added into a 120 mL volumetric flask with approximately 0.02 g of carbon residue; then the systems were kept at 180 °C for 1 h; finally, water was added to make the systems reach 100 mL. 5 mL of the obtained solution was taken for test. Each sample was examined twice under the same conditions, and the data were averaged. The X-ray photoelectron spectroscopy (XPS) spectra of the char residues (surface and inside (cut off the surface layer with thickness of 2 mm)) were recorded with an AXIS ULTRA apparatus (Kratos, England).

■ RESULTS AND DISCUSSION

Synthesis and Characterization of DP1, DP2, EP1, and EP2. In this paper, vanillin was coupled by diamines through Schiff base condensation, and the generated Schiff base further reacted with diethyl phosphite by phosphorus—hydrogen addition reaction to yield phosphorus-containing vanillin-based diphenols DP1 and DP2. Significantly, the Schiff base formation and phosphorus—hydrogen addition reaction were finished in one pot, which means that the Schiff bases produced during the reaction did not need to be extracted from the system. The two phosphorus-containing bio-based epoxy resins EP1 and EP2 were synthesized by reacting DP1 and DP2 with epichlorohydrin by a typical method.

The chemical structures of the synthesized monomers were confirmed by FTIR, ¹H NMR, and ¹³C NMR. Figure 1 presents the FTIR spectra of DP1, DP2, EP1, and EP2. In the FTIR spectra of DP1 and DP2, there are characteristic peaks at

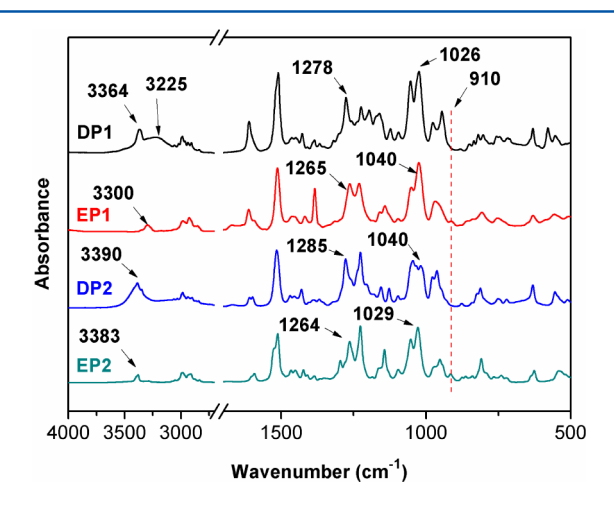


Figure 1. FTIR spectra of DP1, DP2, EP1, and EP2.

3200–3400 cm⁻¹ belonging to N–H and O–H, peaks at around 1280 cm⁻¹ ascribed to P=O, and peaks at around 1030 cm⁻¹ representing P–O. For the FTIR spectra of EP1 and EP2, the peaks for O–H disappeared and the peaks for epoxy group at around 910 cm⁻¹ appeared. As seen from the ¹H NMR and ¹³C NMR spectra of DP1, DP2, EP1, and EP2 (Figures 2 and 3), the chemical shift and integral area of all the peaks match well with the protons and carbons of chemical structures for DP1, DP2, EP1, and EP2. These results indicate that the target compounds were synthesized successfully.

Curing Process. The nonisothermal curing kinetics of EP1-DDM, EP2-DDM, and DGEBA-DDM were studied by DSC. The Kissinger's method (eq 1)^{40–42} and Ozawa's method (eq 2)^{40–43} were used to obtain the apparent activation energy during the curing process.

$$-\ln(q/T_p^2) = E_a/RT_p - \ln(AR/E_a)$$
(1)

$$\ln q = -1.052E_{\rm a}/RT_{\rm p} + \ln(AE_{\rm a}/R) - \ln F(x) - 5.331$$
(2)

where q is the heating rate, $T_{\rm p}$ is the exothermic peak temperature, $E_{\rm a}$ is the activation energy, R is the gas constant, A is the pre-exponential factor, and F(x) is a conversion-dependent term. Figure 4 reveals the plots of $-\ln(q/T_{\rm p}^{\,2})$ versus $1/T_{\rm p}$ based on Kissinger's equation and $\ln q$ versus $1/T_{\rm p}$ based on Ozawa's theory for the EP1-DDM, EP2-DDM, and DER331-DDM systems, and the $E_{\rm a}$ s calculated from the slope of the linear fitting plots are concluded in Table 1. It can be seen that EP1-DDM and EP2-DDM presented similar $E_{\rm a}$ to DGEBA-DDM, which is indicative of the comparable reactivity of EP1 and EP2 to that of DGEBA toward the curing agent DDM.

In order to investigate the curing degree of the systems, FITR spectra of EP1-DDM and EP2-DDM after curing are exhibited in Figure 5. Compared with the FTIR spectra of EP1 and EP2, the peaks for epoxy groups at around 910 cm⁻¹ disappeared and broad peaks ranged from 3200 to 3600 cm⁻¹ representing O–H from the ring-opening reaction between epoxy groups and amines appeared in the FTIR spectra of EP1-DDM and EP2-DDM. This means that the epoxy systems were cured well under the former mentioned conditions.

Flame Retardancy and Flame Retarding Mechanism of the Cured Epoxy Resins. The flame retardancy of the cured epoxy resins was investigated by vertical burning test and limit oxygen index (LOI) examination. The UL-94 ratings and LOI values of the cured epoxy resins are listed in Figure 6. Obviously, the UL-94 V0 rating which was the highest flame retarding rating by vertical burning test was achieved for the EP1-DDM and EP2-DDM systems. Meanwhile, the LOI values of EP1-DDM and EP2-DDM were 31.4% and 32.8%, respectively. Nevertheless, the DGEBA-DDM showed no UL-94 rating and low LOI value of 24.6%. These results illustrate that EP1-DDM and EP2-DDM presented excellent flame retardancy, while DGEBA-DDM was flammable.

Generally, the char residue structure after combustion can reflect the flammability characteristics of polymer materials. Digital photos and SEM photographs of the char residues after LOI test are illustrated in Figure 7, and the phosphorus content in char residues examined by inductively coupled plasma optical emission spectrometer (ICP-OES) is concluded in Table 2. It can be clearly seen in Figure 7a that EP1-DDM and EP2-DDM formed great intumescent char residues, accounting for 35.8% and 41.2% of the original weight of EP1-DDM and EP2-DDM,

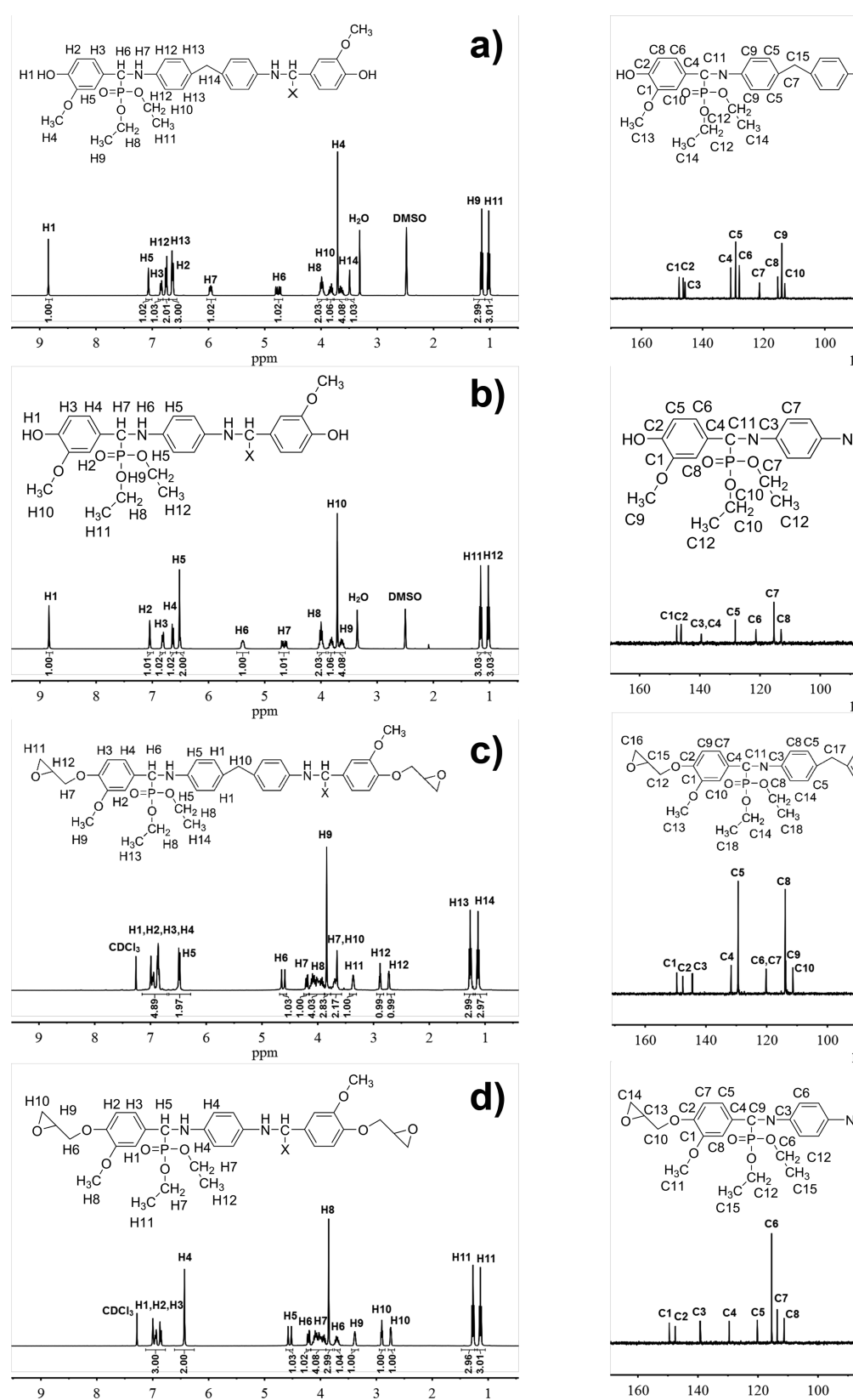


Figure 2. ¹H NMR spectra of (a) DP1, (b) DP2, (c) EP1, and (d) EP2

respectively. Moreover, the char layers of EP1-DDM and EP2-DDM are extremely dense, as shown in Figure 7b. Besides, as shown in Table 2, a large proportion of phosphorus as high as

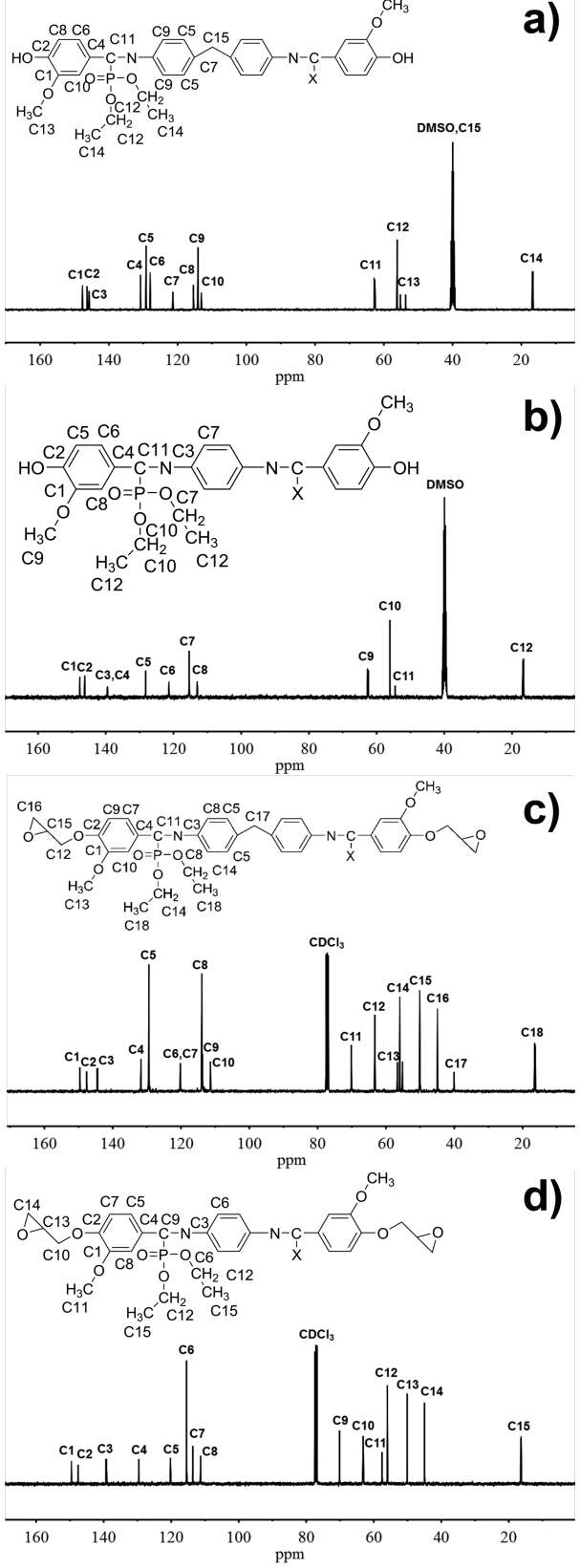


Figure 3. ¹³C NMR spectra of (a) DP1, (b) DP2, (c) EP1, and (d) EP2.

~53.5% was remained in the char, which suggests that the degradation of phosphorus-containing groups produced phosphate structure in the condensed phase and promoted

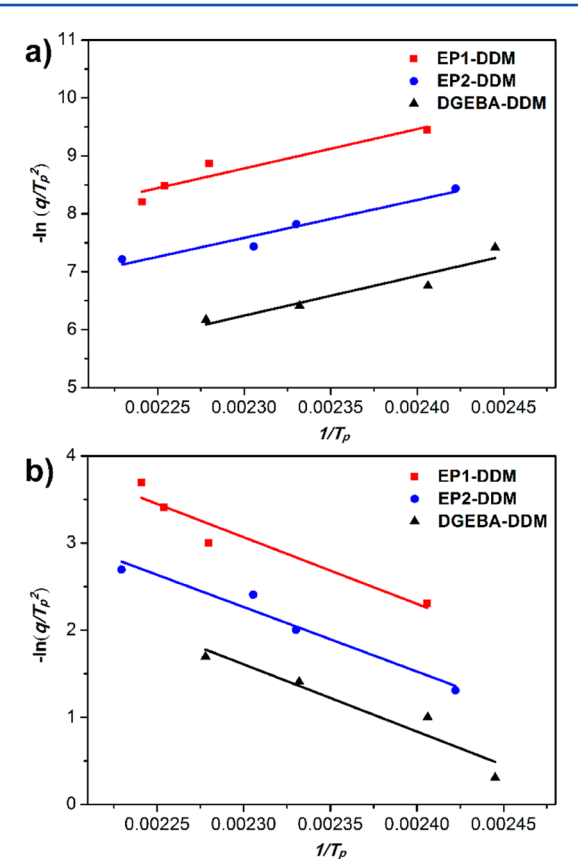


Figure 4. Linear plots of (a) $-\ln(q/T_{\rm p}^{\ 2})$ versus $1/T_{\rm p}$ based on Kissinger's equation and (b) $\ln q$ versus $1/T_{\rm p}$ based on Ozawa's theory.

Table 1. Activation Energy $(E_{\rm a})$ and Average Molecular Weight between Cross-Link Points $(M_{\rm c})$ of EP-DDM, EP2-DDM, and DGEBA-DDM

	E _a (kJ n	nol ⁻¹)	
sample	Kissinger	Ozawa	$M_{ m c}$
EP1-DDM	56.4	60.4	1907
EP2-DDM	54.4	58.5	1727
DGEBA-DDM	57.1	60.9	944

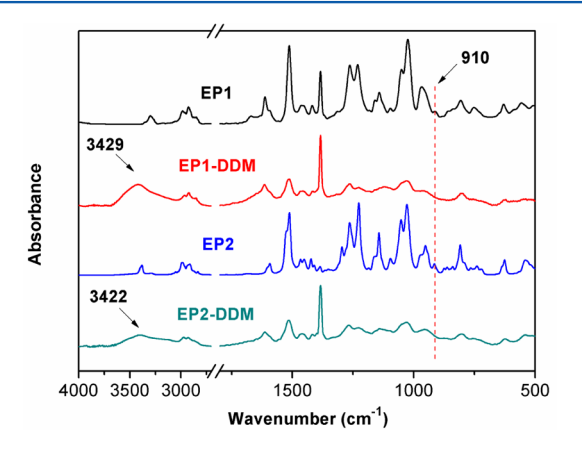


Figure 5. FTIR spectra of the cured EP1-DDM and EP2-DDM.

the configuration of dense char layer to prevent the heat transfer. ^{35,44} Thus, the excellent flame retardancy of EP1-DDM and EP2-DDM was ascribed to their good ability to form

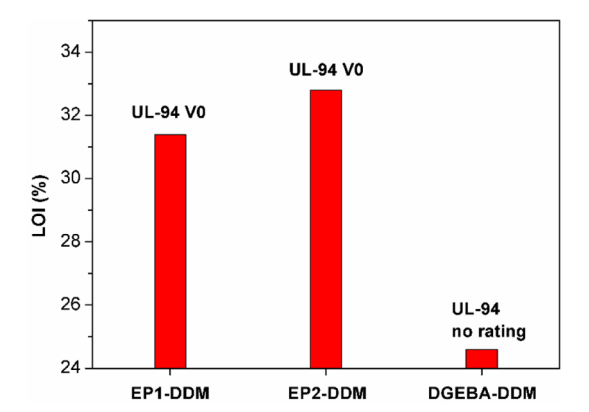


Figure 6. LOI and UL-94 rating of the cured epoxy resins.

intumescent and dense char layers during combustion. While DGEBA-DDM formed a litter bit of char layer with numerous open holes, verifying the failure to prevent the flame and heat transfer. Meanwhile, on account of the more phosphorus and nitrogen content (Table 2), EP2-DDM exhibited better flame retardancy than EP1-DDM reflected from its higher LOI value than EP1-DDM.⁴⁵

To further identify the chemical components of the char residues, the surface part and the inside part of the char residues were examined by XPS, and the XPS spectra are illustrated in Figure 8. Obviously, for both EP1-DDM and EP2-DDM, there are much more phosphorus and oxygen and less carbon in the surface part of the char residues than in the inside part of the char residues. This might be due to the reason that during the combustion the phosphorus transferred to the surface, captured the radicals containing oxygen, and left in the surface layer of the residues, leading to the higher phosphorus and oxygen content in the surface part of char residues for EP1-DDM and EP2-DDM. There is more phosphorus in EP2-DDM than that in EP1-DDM before burning, so there is more phosphorus remained in char residues, and more radicals containing oxygen were captured and remained in the char residues, corresponding to the higher oxygen content of EP2-DDM's char residue than that of EP1-DDM's char residue. Meanwhile, the surface part of char residues had a little higher nitrogen than the inside part of char residues for both EP1-DDM and EP2-DDM, which implies that nitrogen also transferred to the surface of the char residues during the

Thermal Stability. The TGA and DTG curves of the cured epoxy resins under N2 and air atmospheres are illustrated in Figure 9, and the data are summarized in Table 3. As shown in Table 3, EP1-DDM and EP2-DDM exhibited lower degradation temperature for 5% weight loss ($T_{d5\%}$) and higher degradation temperature for 30% weight loss ($T_{\rm d30\%}$) under both atmospheres. The lower $T_{
m d5\%}$ was probably ascribed to the fact that the O=P-O bond in epoxy resin was more apt to degrade than C-C bond. 46 The degradation of the phosphorus containing structure leads to the formation of phosphorus-rich char with high thermal stability, which accumulated at the surface of the epoxy matrix. The thick char was a superior thermal insulating layer, which undergone slow thermal degradation and prevented heat reaching the remaining polymer, 44,47 corresponding to the higher $T_{\rm d30\%}$ of EP1-DDM and EP2-DDM than that of DGEBA-DDM. Although the char layer could be further decomposed with a rise of temperature, 48 the EP1-DDM and EP2-DDM still exhibited much higher char

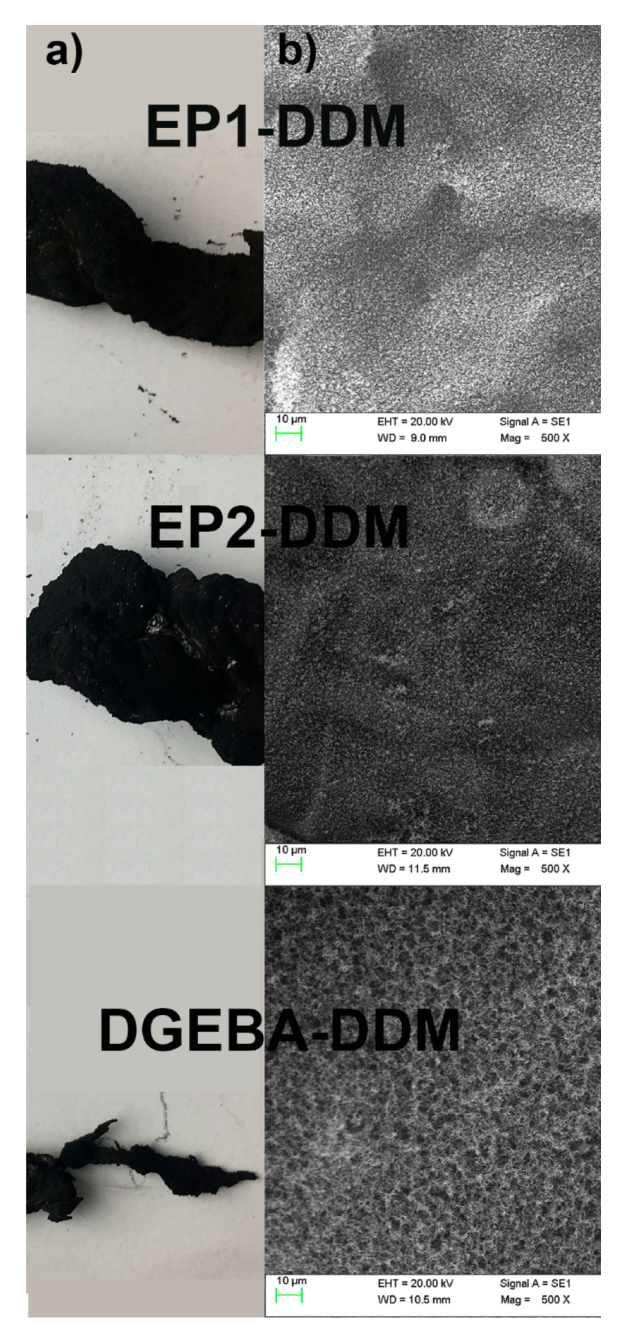


Figure 7. (a) Digital photos and (b) SEM photographs of the residues after LOI test.

yield at 700 °C (R_{700}) as high as ~44.7% under air atmosphere and ~58% under a nitrogen atmosphere than DEGBA-DDM with R_{700} of 0% under air atmosphere and 14.0% under a nitrogen atmosphere. As mentioned previously, the phosphonate group as a promoter for "char formation" formed the phosphorus-rich layer during the degradation process, which

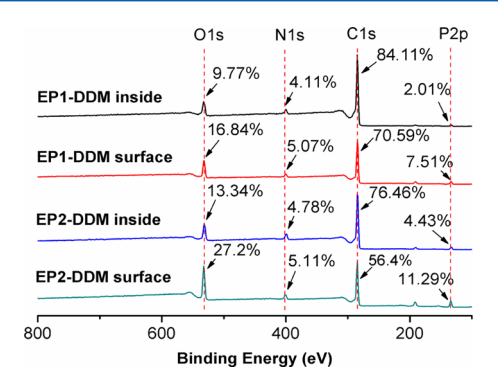


Figure 8. XPS spectra of the surface part and inside part of the char residues of EP1-DDM and EP2-DDM.

resulted in the high char yields. The lower R_{700} under air atmosphere than that under a nitrogen atmosphere was attributed to the third stage degradation belonging to the oxidative degradation of residual carbon under air atmosphere, which can be seen in Figure 9. Meanwhile, the phosphorus content of EP2-DDM is higher than that of EP1-DDM, resulting in its higher $T_{\rm d30\%}$ and R_{700} than EP1-DDM. Higher phosphorus content should lead to lower $T_{\rm d5\%}$ of the phosphorus-containing systems, while EP2-DDM showed higher $T_{\rm d5\%}$ than EP1-DDM. Our previous work proved that increasing the cross-link density can improve the initial degradation temperature. ³⁸ EP2-DDM has higher cross-link density relative to EP1-DDM, which corresponds to its higher $T_{\rm d5\%}$ than EP1-DDM.

Glass Transition Temperature of the Cured Epoxy Resins. Glass transition temperature ($T_{\rm g}$) is a major parameter for thermosetting materials. The $T_{\rm g}$ s of EP1-DDM, EP2-DDM, and DGEBA-DDM were determined by DSC, and the results are summarized in Figure 10. EP1-DDM and EP2-DDM showed higher $T_{\rm g}$ s of 183 and 214 °C, respectively, than DGEBA-DDM with $T_{\rm g}$ of 166 °C. The $T_{\rm g}$ s of the cross-linked polymers have a close tie with their cross-link density and the rigidity of the chain segment structure. The higher the cross-link density of the thermosets and rigidity of their chain segment are the higher the $T_{\rm g}$ is. In order to estimate the cross-link density of the cured epoxy resins, the average molecular weight between cross-link points ($M_{\rm c}$) (Table 1) was calculated using eq 3.

$$M_{\rm c} = \frac{n_{\rm EP} M_{\rm EP} + n_{\rm DDM} M_{\rm DDM}}{n_{\rm DDM}} \tag{3}$$

where n and M represent the molarity and molar mass of the corresponding component in the epoxy formulations. ⁵¹ As shown in Table 1, EP1-DDM and EP2-DDM exhibited higher M_c s than DGEBA-DDM, which means that they possessed lower cross-link density than DGEBA-DDM. Thus, the higher $T_{\rm g}$ s of EP1-DDM and EP2-DDM than that of DGEBA-DDM mainly resulted from the higher rigidity of EP1-DDM and EP2-

Table 2. Phosphorus and Nitrogen Content of EP-DDM, EP2-DDM, and DGEBA-DDM before and after Burning

	before burning		after burning		
sample	phosphorus content (wt %)	nitrogen content (wt %)	weight residue (wt %)	phosphorus content (wt %)	phosphorus retention (%)
EP1-DDM	6.50	4.40	35.8	6.99	38.5
EP2-DDM	7.18	4.86	41.2	9.32	53.5
DGEBA-DDM	0	2.86			

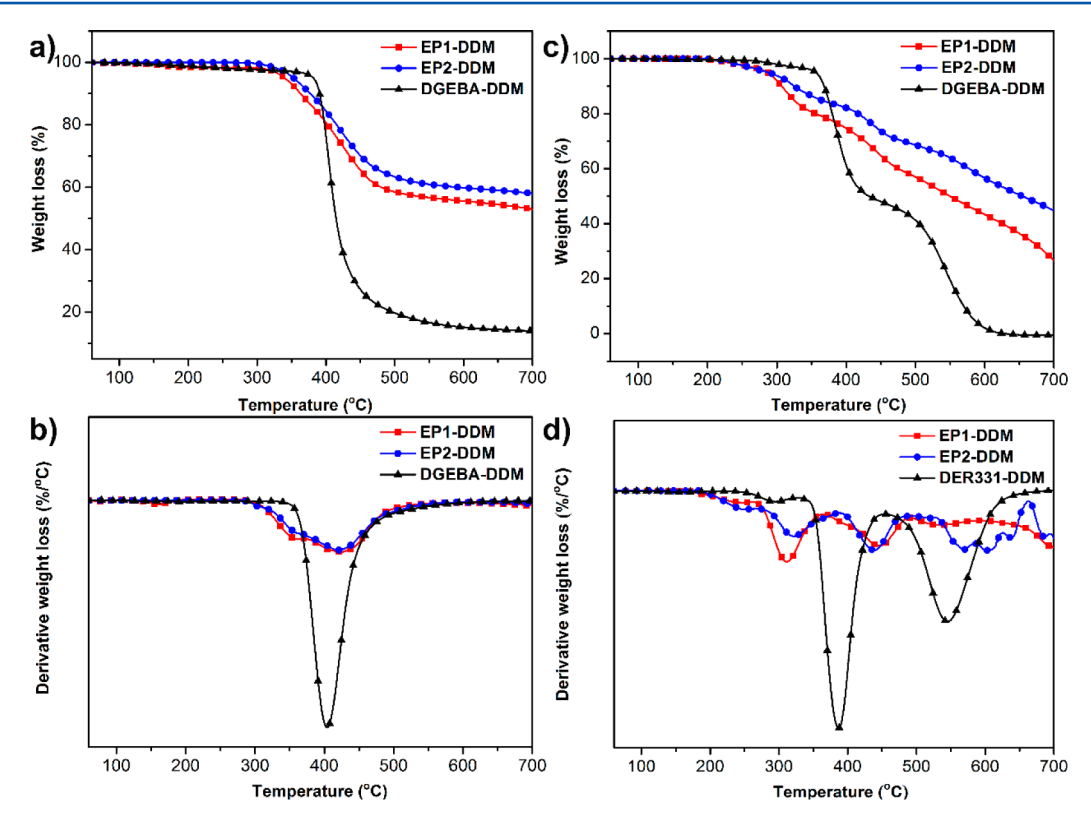


Figure 9. (a) TG and (b) DTG curves under a nitrogen atmosphere and (c) TG and (d) DTG curves under an air atmosphere of the cured epoxy resins.

Table 3. TGA Data of the Cured Epoxy Resins

	$T_{ m d5\%}$	(°C)	$T_{\rm d30\%}$	(°C)	R ₇₀₀	(%)
sample	air	N ₂	air	N ₂	air	N_2
EP1-DDM	286	340	427	435	26.6	53.0
EP2-DDM	287	353	482	450	44.7	58.0
DGEBA-DDM	356	382	390	403	0	14.0

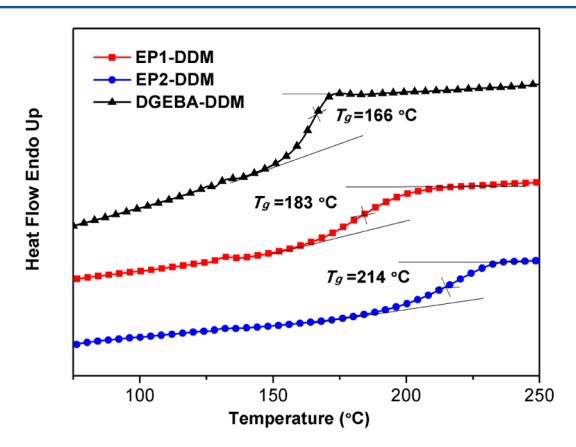


Figure 10. Nonisothermal DSC curves and $T_{\rm g}{\rm s}$ of the cured epoxy resins.

DDM than that of DGEBA-DDM. Although the EP1-DDM and EP2-DDM have flexible phosphate groups $-(P(O)-(O-C_2H_5)_2)$, they possessed more rigid aromatic rings and strongly polar N–H originated intramolecular hydrogen bonds, ^{S2} leading to the higher rigidity of EP1-DDM and EP2-DDM than that of DGEBA-DDM. EP2-DDM displayed lower M_{\odot} corresponding to the higher cross-link density and higher N–H

content than EP1-DDM, resulting in the higher $T_{\rm g}$ of EP2-DDM relative to that of EP1-DDM.

Mechanical Properties. Figure 11 presents the tensile stress-strain curves of the cured epoxies, and their tensile

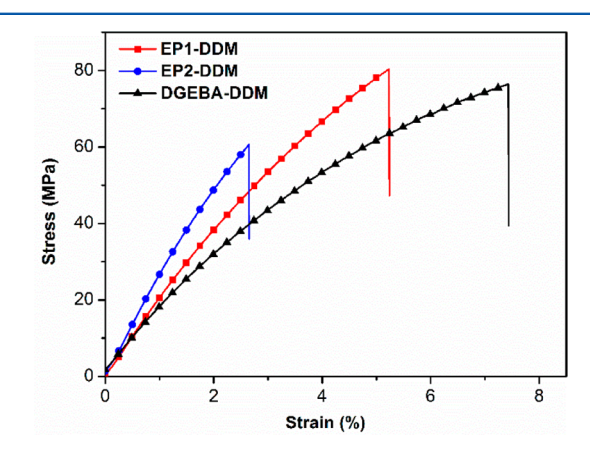


Figure 11. Stress-strain curves for the cured epoxy resins.

properties are summarized in Table 4. All of the epoxy systems exhibited rigid tensile behaviors without a yield point.

Table 4. Mechanical Properties of the Cured Epoxy Resins

sample	tensile strength (MPa)	tensile modulus (MPa)	elongation at break (%)
EP1-DDM	80.3 ± 5	2114 ± 132	5.2 ± 0.4
EP2-DDM	60.6 ± 3	2709 ± 110	2.6 ± 0.2
DGEBA- DDM	76.4 ± 6	1893 ± 140	7.4 ± 0.5

Obviously, the moduli of EP1-DDM and EP2-DDM were much higher than that of the cured DGEBA. As T_g , modulus of thermoset also has a close tie with its cross-link density and rigidity of chain segment structure, 49,50 and the higher moduli of EP1-DDM and EP2-DDM were ascribed to their higher rigidity from the more rigid aromatic rings and strongly polar N-H originated intramolecular hydrogen bonds⁵² than the cured DGEBA. Owing to the higher cross-link density and more N-H of EP2-DDM than those of EP1-DDM and EP2-DDM presented higher modulus than EP1-DDM. The higher rigidity of the EP1-DDM and EP2-DDM led to the lower mobility of the chain segments of the networks, corresponding to the lower elongation at break of the two bio-based epoxy networks than that of DGEBA-DDM. EP2-DDM has higher cross-link density and more N-H originated intramolecular hydrogen bonds than EP1-DDM, resulting in its lower elongation at break than EP1-DDM. Owing to its more strong aromatic rings and N-H originated intramolecular hydrogen bonds, EP1-DDM showed higher tensile strength than DGEBA-DDM. While for the EP2-DDM, it exhibited lower tensile strength than DGEBA-DDM. This is probably due to the more internal stress produced from the curing process for EP2-DDM. The internal stress is related to T_g . When the curing temperature is higher than $T_{g'}$ the internal stress will be low. When the curing temperature is lower than T_g , the internal stress will be high.⁵³ For EP1-DDM and DGEBA-DDM, their $T_{\rm o}$ s are much lower than the curing temperature (230 °C), while the temperature 230 °C locates in the glass transition range of EP2-DDM. As a result, EP2-DDM has high internal stress, leading to the comparatively low tensile strength.

CONCLUSIONS

Two novel bio-based epoxy resins with excellent flame retardancy and thermal and mechanical properties were prepared from the lignin derivative. The epoxy resins were synthesized by the one-pot reaction of Schiff-base structure formation and the phosphorus-hydrogen addition between vanillin, diamines, and diethyl phosphite, followed by the reaction with epichlorohydrin. The bio-based epoxies demonstrated similar curing reactivity to DGEBA. The cured biobased epoxies presented excellent flame retardancy with UL-94 V0 rating and high LOI of 31.4% and 32.8%, which was due to the outstanding intumescent and dense char formation ability. While the commonly used epoxy resin DGEBA was flammable with no UL-94 rating and low LOI of 24.6%. More interestingly, high $T_{\rm g}$ of ~214 °C and outstanding mechanical properties with tensile strength of ~80.3 MPa and tensile modulus of ~2709 MPa, much higher than those of the DGEBA system, were achieved for the bio-based epoxies due to their high rigid structures. Meanwhile, the two bio-based epoxy resins showed different properties due to their different "coupling" structure, which suggested that vanillin-based flame retardant epoxy resins with diverse performance could be easily obtained by adjusting diamines during the synthesis.

AUTHOR INFORMATION

Corresponding Authors

- *(S.M.) E-mail masongqi@nimte.ac.cn; Tel 86-0574-87619806; Fax 86-0574-86685186.
- *(J.Z.) E-mail jzhu@nimte.ac.cn; Tel 86-0574-87619806; Fax 86-0574-86685186.

ORCID ®

Songqi Ma: 0000-0002-9652-1016

Notes

The authors declare no competing financial interest.

ACKNOWLEDGMENTS

The authors are grateful for the financial support from Project 51473180 supported by the National Natural Science Foundation of China, Natural Science Foundation of Zhejiang Province (LY15E030004), and the Ministry for Industry and Information of the People's Republic of China under grant agreement no. [2016] 92.

REFERENCES

- (1) Zhang, Q.; Molenda, M.; Reineke, T. M. Epoxy Resin Thermosets Derived from Trehalose and β -Cyclodextrin. *Macromolecules* **2016**, 49 (22), 8397–8406.
- (2) Vidil, T.; Tournilhac, F.; Musso, S.; Robisson, A.; Leibler, L. Control of reactions and network structures of epoxy thermosets. *Prog. Polym. Sci.* **2016**, *62*, 126–179.
- (3) Auvergne, R.; Caillol, S.; David, G.; Boutevin, B.; Pascault, J.-P. Biobased Thermosetting Epoxy: Present and Future. *Chem. Rev.* **2014**, 114 (2), 1082–1115.
- (4) Song, S. H.; Park, K. H.; Kim, B. H.; Choi, Y. W.; Jun, G. H.; Lee, D. J.; Kong, B. S.; Paik, K. W.; Jeon, S. Enhanced thermal conductivity of epoxy-graphene composites by using non-oxidized graphene flakes with non-covalent functionalization. *Adv. Mater.* **2013**, 25 (5), 732–7.
- (5) Ma, S.; Liu, X.; Jiang, Y.; Tang, Z.; Zhang, C.; Zhu, J. Bio-based epoxy resin from itaconic acid and its thermosets cured with anhydride and comonomers. *Green Chem.* **2013**, *15* (1), 245–254.
- (6) Raquez, J. M.; Deléglise, M.; Lacrampe, M. F.; Krawczak, P. Thermosetting (bio)materials derived from renewable resources: A critical review. *Prog. Polym. Sci.* **2010**, *35* (4), 487–509.
- (7) Ma, S.; Liu, X.; Fan, L.; Jiang, Y.; Cao, L.; Tang, Z.; Zhu, J. Synthesis and Properties of a Bio-Based Epoxy Resin with High Epoxy Value and Low Viscosity. *ChemSusChem* **2014**, 7 (2), 555–562.
- (8) Flint, S.; Markle, T.; Thompson, S.; Wallace, E. Bisphenol A exposure, effects, and policy: A wildlife perspective. *J. Environ. Manage.* **2012**, *104*, 19–34.
- (9) Chrysanthos, M.; Galy, J.; Pascault, J.-P. Preparation and properties of bio-based epoxy networks derived from isosorbide diglycidyl ether. *Polymer* **2011**, 52 (16), 3611–3620.
- (10) Miyagawa, H.; Mohanty, A. K.; Misra, M.; Drzal, L. T. Thermophysical and impact properties of epoxy containing epoxidized linseed oil, 1 Anhydride-cured epoxy. *Macromol. Mater. Eng.* **2004**, 289 (7), 629–635
- (11) Miyagawa, H.; Misra, M.; Drzal, L. T.; Mohanty, A. K. Fracture toughness and impact strength of anhydride-cured biobased epoxy. *Polym. Eng. Sci.* **2005**, 45 (4), 487–495.
- (12) Park, S. J.; Jin, F. L. Synthesis and characterization of UV-curable acrylic resin containing fluorine groups. *Polym. Int.* **2005**, *54* (4), 705–709.
- (13) Park, S. J.; Jin, F. L.; Lee, C. J. Preparation and physical properties of hollow glass microspheres-reinforced epoxy matrix resins. *Mater. Sci. Eng., A* **2005**, 402 (1–2), 335–340.
- (14) Stemmelen, M.; Pessel, F.; Lapinte, V.; Caillol, S.; Habas, J. P.; Robin, J. J. A Fully Biobased Epoxy Resin from Vegetable Oils: From the Synthesis of the Precursors by Thiol-ene Reaction to the Study of the Final Material. *J. Polym. Sci., Part A: Polym. Chem.* **2011**, 49 (11), 2434–2444.
- (15) Dworakowska, S.; Cornille, A.; Bogdał, D.; Boutevin, B.; Caillol, S. Formulation of bio-based epoxy foams from epoxidized cardanol and vegetable oil amine. *Eur. J. Lipid Sci. Technol.* **2015**, *117* (11), 1893–1902.
- (16) Feng, X. H.; East, A. J.; Hammond, W. B.; Zhang, Y.; Jaffe, M. Overview of advances in sugar-based polymers. *Polym. Adv. Technol.* **2011**, 22 (1), 139–150.

(17) Liu, X. Q.; Zhang, J. W. High-performance biobased epoxy derived from rosin. *Polym. Int.* **2010**, *59* (5), 607–609.

- (18) Liu, X. Q.; Huang, W.; Jiang, Y. H.; Zhu, J.; Zhang, C. Z. Preparation of a bio-based epoxy with comparable properties to those of petroleum-based counterparts. *eXPRESS Polym. Lett.* **2012**, *6* (4), 293–298.
- (19) Aouf, C.; Lecomte, J.; Villeneuve, P.; Dubreucq, E.; Fulcrand, H. Chemo-enzymatic functionalization of gallic and vanillic acids: synthesis of bio-based epoxy resins prepolymers. *Green Chem.* **2012**, 14 (8), 2328–2336.
- (20) Aouf, C.; Nouailhas, H.; Fache, M.; Caillol, S.; Boutevin, B.; Fulcrand, H. Multi-functionalization of gallic acid. Synthesis of a novel bio-based epoxy resin. *Eur. Polym. J.* **2013**, 49 (6), 1185–1195.
- (21) Cao, L.; Liu, X.; Na, H.; Wu, Y.; Zheng, W.; Zhu, J. How a biobased epoxy monomer enhanced the properties of diglycidyl ether of bisphenol A (DGEBA)/graphene composites. *J. Mater. Chem. A* **2013**, *1* (16), 5081–5088.
- (22) Ménard, R.; Caillol, S.; Allais, F. Ferulic acid-based renewable esters and amides-containing epoxy thermosets from wheat bran and beetroot pulp: Chemo-enzymatic synthesis and thermomechanical properties characterization. *Ind. Crops Prod.* **2017**, *95*, 83–95.
- (23) Koike, T. Progress in Development of Epoxy Resin Systems Based on Wood Biomass in Japan. *Polym. Eng. Sci.* **2012**, 52 (4), 701–717.
- (24) Zhao, B.; Chen, G.; Liu, Y.; Hu, K.; Wu, R. Synthesis of lignin base epoxy resin and its characterization. *J. Mater. Sci. Lett.* **2001**, 20 (9), 859–862.
- (25) Fache, M.; Viola, A.; Auvergne, R.; Boutevin, B.; Caillol, S. Biobased epoxy thermosets from vanillin-derived oligomers. *Eur. Polym. J.* **2015**, *68* (0), 526–535.
- (26) Fache, M.; Auvergne, R.; Boutevin, B.; Caillol, S. New vanillinderived diepoxy monomers for the synthesis of biobased thermosets. *Eur. Polym. J.* **2015**, *67*, 527–538.
- (27) Chrysanthos, M.; Galy, J.; Pascault, J.-P. Influence of the Bio-Based Epoxy Prepolymer Structure on Network Properties. *Macromol. Mater. Eng.* **2013**, 298 (11), 1209–1219.
- (28) Łukaszczyk, J.; Janicki, B.; Kaczmarek, M. Synthesis and properties of isosorbide based epoxy resin. *Eur. Polym. J.* **2011**, 47 (8), 1601–1606.
- (29) Tuck, C. O.; Pérez, E.; Horváth, I. T.; Sheldon, R. A.; Poliakoff, M. Valorization of Biomass: Deriving More Value from Waste. *Science* **2012**, 337 (6095), 695–699.
- (30) Upton, B. M.; Kasko, A. M. Strategies for the Conversion of Lignin to High-Value Polymeric Materials: Review and Perspective. *Chem. Rev.* **2016**, *116* (4), 2275–2306.
- (31) Hofmann, K.; Glasser, W. Engineering plastics from lignin, 23. Network formation of lignin-based epoxy resins. *Macromol. Chem. Phys.* **1994**, *195* (1), 65–80.
- (32) Hofmann, K.; Glasser, W. G. Engineering Plastics from Lignin. 22. Cure of Lignin Based Epoxy Resins. *J. Adhes.* **1993**, *40* (2–4), 229–241.
- (33) Fache, M.; Boutevin, B.; Caillol, S. Vanillin, a key-intermediate of biobased polymers. *Eur. Polym. J.* **2015**, *68*, 488–502.
- (34) Fache, M.; Darroman, E.; Besse, V.; Auvergne, R.; Caillol, S.; Boutevin, B. Vanillin, a promising biobased building-block for monomer synthesis. *Green Chem.* **2014**, *16* (4), 1987–1998.
- (35) Liu, Y. L. Flame-retardant epoxy resins from novel phosphorus-containing novolac. *Polymer* **2001**, *42* (8), 3445–3454.
- (36) Qian, X.; Song, L.; Bihe, Y.; Yu, B.; Shi, Y.; Hu, Y.; Yuen, R. K. Organic/inorganic flame retardants containing phosphorus, nitrogen and silicon: preparation and their performance on the flame retardancy of epoxy resins as a novel intumescent flame retardant system. *Mater. Chem. Phys.* **2014**, *143* (3), 1243–1252.
- (37) The European Parliament and the European Council: Off. J. Eur. Union, 2003, Directive 2002/96/EC of 27.
- (38) Ma, S.; Liu, X.; Jiang, Y.; Fan, L.; Feng, J.; Zhu, J. Synthesis and properties of phosphorus-containing bio-based epoxy resin from itaconic acid. *Sci. China: Chem.* **2014**, *57* (3), 379–388.

(39) Illy, N.; Fache, M.; Ménard, R.; Negrell, C.; Caillol, S.; David, G. Phosphorylation of bio-based compounds: the state of the art. *Polym. Chem.* **2015**, *6* (35), *6*257–*6*291.

- (40) Roşu, D.; Caşcaval, C.; Mustată, F.; Ciobanu, C. Cure kinetics of epoxy resins studied by non-isothermal DSC data. *Thermochim. Acta* **2002**, 383 (1), 119–127.
- (41) Cai, H.; Li, P.; Sui, G.; Yu, Y.; Li, G.; Yang, X.; Ryu, S. Curing kinetics study of epoxy resin/flexible amine toughness systems by dynamic and isothermal DSC. *Thermochim. Acta* **2008**, 473 (1–2), 101–105.
- (42) Wang, C. S.; Lin, C. H. Properties and curing kinetic of diglycidyl ether of bisphenol A cured with a phosphorus-containing diamine. *J. Appl. Polym. Sci.* **1999**, *74* (7), 1635–1645.
- (43) Wang, Q.; Shi, W. Kinetics study of thermal decomposition of epoxy resins containing flame retardant components. *Polym. Degrad. Stab.* **2006**, 91 (8), 1747–1754.
- (44) Qian, L.; Qiu, Y.; Sun, N.; Xu, M.; Xu, G.; Xin, F.; Chen, Y. Pyrolysis route of a novel flame retardant constructed by phosphaphenanthrene and triazine-trione groups and its flame-retardant effect on epoxy resin. *Polym. Degrad. Stab.* **2014**, *107*, 98–105.
- (45) Wang, Y.; Zhao, J.; Yuan, Y.; Liu, S.; Feng, Z.; Zhao, Y. Synthesis of maleimido-substituted aromatic s-triazine and its application in flame-retarded epoxy resins. *Polym. Degrad. Stab.* **2014**, *99*, 27–34.
- (46) Wang, X.; Song, L.; Xing, W.; Lu, H.; Hu, Y. A effective flame retardant for epoxy resins based on poly(DOPO substituted dihydroxyl phenyl pentaerythritol diphosphonate. *Mater. Chem. Phys.* **2011**, *125* (3), *536*–541.
- (47) Xu, W.; Wirasaputra, A.; Liu, S.; Yuan, Y.; Zhao, J. Highly effective flame retarded epoxy resin cured by DOPO-based co-curing agent. *Polym. Degrad. Stab.* **2015**, *122*, 44–51.
- (48) Wang, X.; Hu, Y.; Song, L.; Xing, W.; Lu, H. Thermal degradation mechanism of flame retarded epoxy resins with a DOPO-substitued organophosphorus oligomer by TG-FTIR and DP-MS. *J. Anal. Appl. Pyrolysis* **2011**, 92 (1), 164–170.
- (49) Ma, S.; Webster, D. C. Naturally Occurring Acids as Cross-Linkers To Yield VOC-Free, High-Performance, Fully Bio-Based, Degradable Thermosets. *Macromolecules* **2015**, 48 (19), 7127–7137.
- (50) Ma, S.; Webster, D. C.; Jabeen, F. Hard and Flexible, Degradable Thermosets from Renewable Bioresources with the Assistance of Water and Ethanol. *Macromolecules* **2016**, 49 (10), 3780–3788.
- (51) Xie, T.; Rousseau, I. A. Facile tailoring of thermal transition temperatures of epoxy shape memory polymers. *Polymer* **2009**, *50* (8), 1852–1856.
- (52) Liu, H.; Xu, K.; Cai, H.; Su, J.; Liu, X.; Fu, Z.; Chen, M. Thermal properties and flame retardancy of novel epoxy based on phosphorus-modified Schiff-base. *Polym. Adv. Technol.* **2012**, 23 (1), 114–121.
- (53) Chen, Z.-K.; Yang, G.; Yang, J.-P.; Fu, S.-Y.; Ye, L.; Huang, Y.-G. Simultaneously increasing cryogenic strength, ductility and impact resistance of epoxy resins modified by n-butyl glycidyl ether. *Polymer* **2009**, *50* (5), 1316–1323.